11-11-2009

A dimensionless number describing the effects of recharge and geometry on discharge from simple karstic aquifers

M. D. Covington

C. M. Wicks

M. O. Saar

A dimensionless number describing the effects of recharge and geometry on discharge from simple karstic aquifers

M. D. Covington,[1] C. M. Wicks,[2] and M. O. Saar[1]

Received 19 March 2009; revised 29 June 2009; accepted 13 August 2009; published 11 November 2009.

[1] The responses of karstic aquifers to storms are often used to obtain information about aquifer geometry. In general, spring hydrographs are a function of both system geometry and recharge. However, the majority of prior work on storm pulses through karst has not studied the effect of recharge on spring hydrographs. To examine the relative importance of geometry and recharge, we break karstic aquifers into elements according to the manner of their response to transient flow and demonstrate that each element has a characteristic response timescale. These fundamental elements are full pipes, open channels, reservoir/constrictions, and the porous matrix. Taking the ratio of the element timescale with the recharge timescale produces a dimensionless number, γ, that is used to characterize aquifer response to a storm event. Using sets of simulations run with randomly selected element parameters, we demonstrate that each element type has a critical value of γ below which the shape of the spring hydrograph is dominated by the shape of the recharge hydrograph and above which the spring hydrograph is significantly modified by the system geometry. This allows separation of particular element/storm pairs into recharge-dominated and geometry-dominated regimes. While most real karstic aquifers are complex combinations of these elements, we draw examples from several karst systems that can be represented by single elements. These examples demonstrate that for real karstic aquifers full pipe and open channel elements are generally in the recharge-dominated regime, whereas reservoir/constriction elements can fall in either the recharge- or geometry-dominated regimes.

Citation: Covington, M. D., C. M. Wicks, and M. O. Saar (2009), A dimensionless number describing the effects of recharge and geometry on discharge from simple karstic aquifers, *Water Resour. Res.*, *45*, W11410, doi:10.1029/2009WR008004.

1. Introduction

[2] The central difficulty in karst hydrology is that the geometry of the conduit network within most karstic aquifers is poorly known, and that these unknown conduits control the flow through the aquifer. Additionally, conduit network geometry is difficult to determine using geophysical techniques from the surface, as there is a trade-off between the size of the feature that can be imaged and the depth below the land surface at which the feature lies [*Benson et al.*, 2003; *Yuhr*, 2009]. Therefore, any means by which we can gain information about a karstic aquifer via external hydrological monitoring is potentially very useful. Monitoring the response of karstic aquifers to storms is one of the main techniques that has been applied. The bulk of the previous work on storm pulses in karstic aquifers can be grouped into those studies that analyze rainfall-spring discharge relations [e.g., *Ashton*, 1966; *Brown*, 1970; *Knisel*, 1972; *Brown*, 1973; *Dreiss*, 1982; *Labat et al.*, 2000a, 2000b; *Denic-Jukic and Jukic*, 2003; *Panagopoulos and Lambrakis*, 2006] and those studies that attempt to ascertain the properties of the aquifer through characterization of the hydrographs, sometimes complemented by chemographs or thermographs [e.g., *Dreiss*, 1983; *Eisenlohr et al.*, 1997; *Kiraly et al.*, 1995; *Grasso and Jeannin*, 2002; *Grasso et al.*, 2003; *Birk et al.*, 2004; *Kovács et al.*, 2005; *Birk et al.*, 2006].

[3] The underlying concept of the latter group of work is that as a storm pulse propagates through the aquifer, the storm pulse is altered, these alterations are recorded in the spring hydrographs, and deciphering the hydrographs provides information about the aquifer geometry (Figure 1a). These studies have interpreted spring hydrographs in terms of the gross properties of a karstic aquifer. *Dreiss* [1983] used linear transfer functions to define the spring shed (area of land that drains water to a spring) of Big Spring in Missouri. *Kiraly et al.* [1995] focused on the role of epikarst in effecting the shape of the hydrographs. *Grasso et al.* [2003] used two parameters to characterize system responses: one a function of the geometry of saturated conduits, and the other a function of the degree to which water was undersaturated with respect to calcite. *Birk et al.* [2004, 2006] have shown that global aquifer parameters may be estimated using time lags between hydrographs, thermographs, and chemographs measured at the spring. *Kovács et al.* [2005] studied the recession hydrographs of two-dimensional networks of conduits embedded in a porous matrix and demonstrated that recession from mature

[1]Department of Geology and Geophysics, University of Minnesota-Twin Cities, Minneapolis, Minnesota, USA.
[2]Department of Geology and Geophysics, Louisiana State University, Baton Rouge, Louisiana, USA.

0043-1397/09/2009WR008004

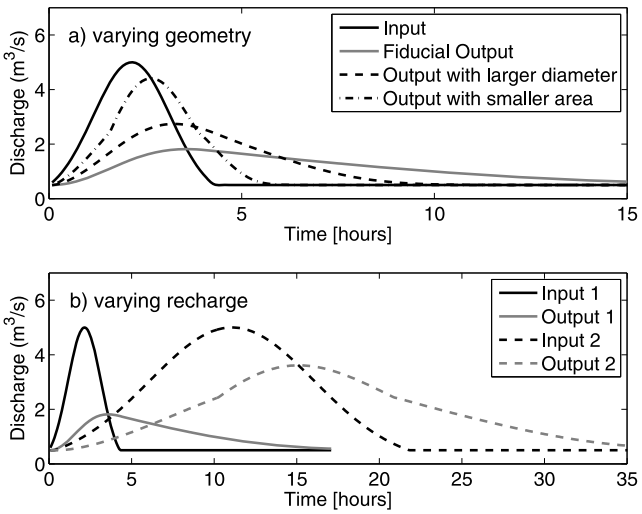

Figure 1. Examples of simulated spring discharge hydrographs as controlled (a) by aquifer geometry and (b) by recharge hydrographs. The hydrographs depicted are inputs and outputs simulated for reservoir/constriction systems with the geometrical parameters varied in Figure 1a and the storm duration varied in Figure 1b. For Figure 1a, a fiducial output is shown, along with a case with a larger diameter constriction (dashed line) and another case with a smaller reservoir surface area (dash-dotted line). The depicted system responses demonstrate that both the geometry and the recharge can have significant effects on the shape of the output.

karst systems is typically determined by the matrix component of the system. The matrix recession is in general a function of the size and properties of the blocks between conduits. *Hergarten and Birk* [2007] extended this work to demonstrate that the recession is actually a function of the size distribution of blocks, with the small blocks determining early recession and the large blocks determining late recession. Additional work on the relation between discharge and geometry established that conduit-dominated systems result in sharply peaked discharge curves whereas rock matrix-dominated systems result in broader curves [*Florea and Vacher*, 2006]. Nevertheless, much remains to be learned about how the effects of conduit geometry are reflected in spring hydrographs.

[4] Spring hydrographs should also reflect the characteristics of the input storm pulse (Figure 1b). Intuitively, for a simple cave stream with large conduits it is probable that the spring hydrograph is almost entirely dependent on the input and that the geometry of the cave stream produces a negligible modification of the storm pulse. Conversely, complex systems of constrictions and reservoirs (conduits draining ponded water) can be expected to drastically modify the input storm pulse. This is a complicating factor that many of the previous studies have not explored in detail. However, *Eisenlohr et al.* [1997] suggested that the shape of spring hydrographs are a function of the structure of the aquifer, the form of the floods, the frequency of storm events, and the type of infiltration. *Grasso and Jeannin* [2002] interpret hydrographs and chemographs in terms of both aquifer structure and bioclimatic variables. The previously cited group of studies that focused on rainfall-discharge relations used rainfall as the input signal even in cases where the actual input signal is a losing stream or lake. In these cases, the rainfall signal has been modified by surface processes [e.g., *Tessier et al.*, 1996].

[5] Important questions are: To what extent is the discharge a function of the characteristics of the recharge as opposed to the characteristics of the aquifer geometry? Under what conditions does either recharge pattern or geometry play a dominant role in determining discharge characteristics? Is it possible to separate the effects of recharge and geometry? Therefore, the goal of this study is to delineate the regime in which a spring hydrograph is largely a function of input and the regime in which a spring hydrograph is largely a function of aquifer geometry. Using models of simple karstic aquifers, this work investigates how storm pulses are modified by the properties of the aquifer and to what extent the spring hydrograph resembles the input hydrograph. *Geyer et al.* [2008] also compared recharge and discharge hydrographs using a dual linear reservoir model of a karstic aquifer. Our work differs from theirs in that they assume a simplified lumped parameter model for the whole aquifer, whereas we try to understand the fundamental physics that governs the response of the small elements that make up a karstic aquifer.

2. Elements of Karstic Aquifers

[6] Traditionally, karstic aquifers are modeled as a network of open conduits embedded in both a system of fractures and a porous rock matrix [*Torbarov*, 1976; *Milanovic*, 1976; *Birk et al.*, 2006; *Kaufmann*, 2009; S. D. C. Walsh and M. O. Saar, Macroscale lattice-Boltzmann methods for solute and heat transport in heterogeneous porous, fractured, and conduit media, submitted to *Water Resources Research*, 2009]. However, for the purposes of studying storm pulses through karstic aquifers, it is useful to refine this characterization. First, we split the system of conduits into three different types, or elements, 1) pipe-full, 2) open channels, and 3) reservoirs up gradient from a constriction. Each of these conduit types responds quite differently to transient flow. Second, while the magnitude and timescale of rock matrix and fracture responses may differ, the nature of their responses is similar. Thus, we combine the rock matrix and the fracture porosities in which the conduits are embedded into a single element that we call 'matrix' hereafter.

[7] Another important consideration is how one defines the input into the model. Input from rainfall can be modified via surface processes, infiltration through soil, and flow through the epikarst before reaching the conduit network. In the work that follows, to avoid this additional complexity, we use the input directly into the conduit network, rather than rainfall, as the input into our models.

[8] As mentioned above, conduits in a karstic aquifer can act in three different modes. The first, and simplest, mode is full-pipe flow (Figure 2a) [*Brown*, 1973]. For a single section of conduit that is completely filled with water, $R(t) = Q(t)$, where $R(t)$ and $Q(t)$ are the time dependent volume fluxes into and out of the conduit, respectively. Thus, the geometry of the pipe section does not modify the shape of a flood pulse and any delay between $R(t)$ and $Q(t)$ is minor.

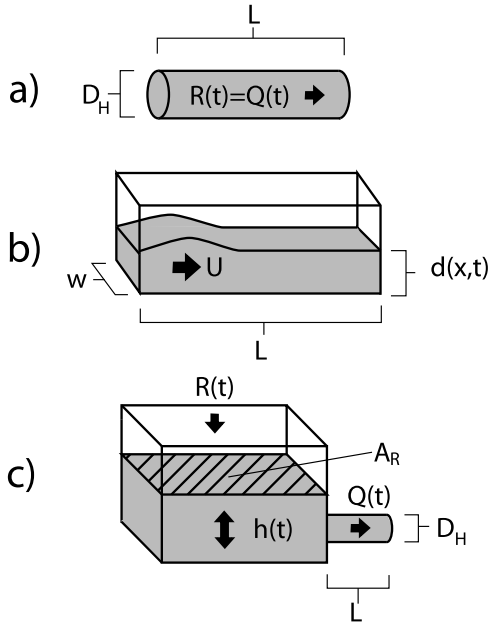

Figure 2. Modes of conduit flow in karstic aquifers that process flood pulses in different manners: (a) full pipes, (b) open channels, and (c) reservoir/constrictions. For full pipes, at any given time the flux into the element is equal to the flux out. For the open channel and reservoir/constriction this need not be the case since they contain free surfaces. Symbols are defined in the main text.

[9] In contrast, a conduit that is only partially filled with water behaves in a more complex fashion. This open channel flow is analogous to a surface stream [*Stoker*, 1957; *Henderson*, 1963; *Ponce and Simons*, 1977; *Ferrick*, 1985]. A storm pulse propagating down an open channel (Figure 2b) can be modified as the free surface in the conduit allows the volume of water in the conduit section to vary with time. This results in a time lag between $R(t)$ and $Q(t)$. Furthermore, the pressure field of the storm pulse slowly diffuses as it moves down the channel, allowing the shapes of the input and output hydrographs to vary.

[10] The final mode in which a conduit can act is as a drain to a reservoir. This occurs when a constriction in the aquifer results in the ponding of water upstream of the constriction (Figure 2c) [*Halihan and Wicks*, 1998]. The constricted portion of the system operates as a full pipe, whereas the larger upstream portion of the conduit provides a reservoir with a free surface that can fill and drain through the course of a flood event.

[11] A karst conduit network is also typically embedded in a porous matrix. The permeability of the matrix portion of the system is assumed to be sufficiently low that the effect on the short-term storm response is small. Specifically, *Peterson and Wicks* [2005] showed for a particular set of example cases that the volume of water that flows into the porous matrix during a storm pulse is quite small compared to flow through the conduits. However, during the recession flow of the spring, it is possible that the matrix provides a significant portion of the discharge. This flow would be a combination of flood water drainage from the matrix and diffuse recharge water that entered through the matrix instead of directly into a conduit. *Geyer et al.* [2008] illustrate the effect on system response when a significant portion of the recharge enters through the matrix rather than directly into the conduit network.

3. Characteristic Response Times

[12] Each of the karstic aquifer elements described previously has a characteristic response timescale. That is, if we perturb a system element away from equilibrium by changing the boundary conditions, then there is a timescale over which the flow changes and approaches a new equilibrium for the new boundary conditions. This timescale will be a function of both the geometrical parameters of the element and the amount by which we perturb the system. Such timescales are useful because if boundary conditions are changing very slowly with respect to the system timescale, then the system can be well approximated by ignoring transient effects and calculating the system state at every point in time assuming equilibrium. This results because the system can adjust to equilibrium faster than the change in boundary conditions. For a karstic aquifer element, this assumption of equilibrium equates to an assumption that the recharge into the element is equal to the discharge from the element, and in this case the discharge from the element is clearly determined by the recharge and not the geometry.

[13] Previous work has noted characteristic times of karstic aquifers, for example the recession coefficient. However, most of the work on such characteristics has focused on lumped parameter or black box models, in which the connection between the recession time and the geometry of the system is not necessarily clear. We take the opposite approach and begin with the smallest pieces of a karstic aquifer in order to understand what determines the time over which an element of the aquifer will respond. In the following sections we derive these response timescales for each element type and define a characteristic recharge timescale. These element timescales are used in Section 4 along with recharge timescales in order to delineate the effects of geometry and recharge on system response. In all cases, we assume that the rock matrix is incompressible.

3.1. Full Pipes

[14] Neglecting the compressibility of water, which is small, full pipe flow (Figure 2a) must conserve mass such that $R(t) = Q(t)$. Nevertheless, for changes in head boundary conditions, full pipes retain a finite response time. That is, if the head boundary condition is changed, the resultant change in flow does not occur instantaneously. This delay results from two mechanisms. First, it takes a finite amount of time for the pressure wave to propagate through the conduit. Unlike pressure waves in Darcian aquifers [*Saar and Manga*, 2003], pressure waves in conduits propagate with a speed comparable to the sound speed in open water ($\sim$1500 m s^{-1}). Thus, the pressure wave timescale of the system is roughly equal to the length of the conduit divided by the sound speed in water. In comparison to typical timescales of recharge events, this response time is so small as to be inconsequential.

[15] The second mechanism for delay is the momentum of the water. When the head boundary conditions change, the column of water in the pipe must gain inertia and

accelerate to the new flow velocity that satisfies the new pressure gradient. Treating the column of water in a full pipe as a rigid body, such that the average velocity of the water in the pipe is constant along the length of the pipe, and applying Newton's second law to that column of water results in Euler's equation for one-dimensional fluid flow through a pipe [*Larock et al.*, 2000, equation (7.16)].

$$-\frac{1}{\rho g}\frac{\partial P}{\partial x}-\frac{\partial z}{\partial x}-\frac{4\tau_0}{\rho g D_{\mathrm{H}}}=\frac{1}{g}\frac{dV}{dt}, \tag{1}$$

where x is the dimension along the length of the pipe, t is time, V is the average velocity in the pipe, z is the elevation of the pipe as a function of x, P is the pressure as a function of x, D_{H} is the hydraulic diameter of the pipe, τ_0 is the shear stress between the fluid and the wall, ρ is the density of water, and g is Earth's gravitational acceleration. Substituting in the Darcy-Weisbach friction factor, f, for τ_0 using

$$\tau_0=\frac{1}{8}F\rho V|V| \tag{2}$$

and the hydraulic head

$$h=\frac{P}{\rho g}+z \tag{3}$$

and assuming that $V = V(t)$ is constant along the length of the conduit, equation (1) can be written as

$$\frac{1}{g}\frac{\partial V}{\partial t}+\frac{\partial h}{\partial x}+\frac{f}{D_{\mathrm{H}}}\frac{V|V|}{2g}=0. \tag{4}$$

Equation (4) can be integrated along the length of the conduit to obtain

$$\frac{L}{g}\frac{dV}{dt}+\frac{fL}{D_{\mathrm{H}}}\frac{V|V|}{2g}=h_{\mathrm{in}}, \tag{5}$$

where L is the length of the conduit, h_{in} is the hydraulic head at the upstream boundary of the conduit, and the downstream head is set to zero.

[16] In order to derive the characteristic response time for the system, we consider a hypothetical conduit with an initial flow velocity of zero. At time $t = 0$ the hydraulic head at the upstream end is instantaneously increased to some constant value h_{f}. In order to solve for the equilibrium flow velocity in the system once it has responded to the new head boundary condition, we set the acceleration term in equation (5) to zero, resulting in the Darcy-Weisbach Equation for steady flow through a pipe [*Larock et al.*, 2000, equation (2.10)],

$$V_{\mathrm{f}}^2=\frac{2gD_{\mathrm{H}}}{fL}h_{\mathrm{f}}. \tag{6}$$

f is calculated from the empirically derived Colebrook-White equation [*Larock et al.*, 2000, equation (2.21)],

$$\frac{1}{\sqrt{f}}=-2\log\left(\frac{\epsilon}{3.7D_{\mathrm{H}}}+\frac{2.51}{Re\sqrt{f}}\right), \tag{7}$$

where ϵ is the wall roughness and Re is the Reynolds number. In general, f is a function of both pipe properties and the degree of turbulence in the flow. However, for natural karst conduits flow is likely to be turbulent for cases with a hydraulic diameter larger than 1 cm [*White*, 1988, Figure 6.10]. In our model, conduits or fractures that are smaller than this diameter and transmit laminar flow are considered to be a part of the matrix component of the system. For laminar flow, the discharge is linearly proportional to the head drop. Therefore, the dynamics of small laminar flow conduits are analogous to the dynamics of the Darcian flow in the porous matrix, and a characteristic time for a laminar flow conduit could be derived in a way similar to the matrix timescale of Section 3.4. However, for the main conduit flow paths in karstic aquifers Re will be large, and thus the second term in the logarithm of equation (7) is small. If this term is neglected then f is constant over the range of flows experienced, and equation (5) can be separated to obtain

$$dt=\frac{LdV}{g(h-fLV|V|/2gD_{\mathrm{H}})}. \tag{8}$$

Finally, integrating from 0 to t and substituting in V_{f} from equation (6) results in

$$t=\frac{D_{\mathrm{H}}}{fV_{\mathrm{f}}}\ln\left(\frac{V_{\mathrm{f}}+V}{V_{\mathrm{f}}-V}\right), \tag{9}$$

where V_{f} is the equilibrium velocity for the new head difference, h_{f}. The equation shows that the velocity, V, asymptotes to V_{f} as $t \rightarrow \infty$ with a characteristic time scale of

$$\tau_{\mathrm{mom}}\sim\frac{D_{\mathrm{H}}}{fV_{\mathrm{f}}}. \tag{10}$$

[17] For natural karst conduits, the full pipe response time will typically be small compared to the timescale of recharge events. The pressure wave timescale of the system is roughly equal to the length of the conduit divided by the sound speed in water, and is much shorter than the momentum response time. Furthermore, the momentum response time will typically be short enough to be negligible. For example, a conduit one meter in diameter, with a friction coefficient of $f \sim 0.05$, and a peak flow velocity of one meter per second would have a momentum response time of only $\tau_{\mathrm{mom}} = 20$ sec.

3.2. Open Channels

[18] One-dimensional open channel flow (Figure 2b) is governed by the Saint Venant equations [*Stoker*, 1957; *Chanson*, 2004] which include a momentum equation,

$$\frac{1}{g}\left(\frac{\partial V}{\partial t}+V\frac{\partial V}{\partial x}\right)+\frac{\partial d}{\partial x}+S_{\mathrm{f}}-S_0=0, \tag{11}$$

and a continuity equation,

$$\frac{\partial A}{\partial t}+\frac{\partial Q}{\partial x}=0, \tag{12}$$

where $V(x, t)$ is the flow velocity, $d(x, t)$ is the flow depth,

$$S_f = \frac{f}{2gD_H} V|V| \tag{13}$$

is the friction slope, quantifying the frictional head loss along the length of the channel, S_0 is the slope of the channel bottom, $A(x, t)$ is the cross-sectional area of the flow, and $Q(x, t)$ is the flow rate.

[19] Two common approximations for unsteady open channel flow are the kinematic wave approximation and the diffusion wave approximation [*Ponce and Simons*, 1977; *Ferrick*, 1985]. For both of these approximations the acceleration and inertial terms (the two terms in parentheses in equation (11)) are assumed to be negligible. For the kinematic wave, the free surface is also presumed to be parallel to the channel bottom and therefore $\partial d/\partial x = 0$.

[20] Thus, the kinematic wave equation is simply

$$S_f = S_0. \tag{14}$$

Substituting in the definition of the friction slope (equation (13)), and the channel slope ($\Delta z/L$) simply results in a form of the Darcy-Weisbach equation,

$$\Delta h = \frac{fL}{2gD_H} V|V|. \tag{15}$$

Therefore, the average flow velocity during kinematic wave propagation is calculated using the relation for equilibrium flow. Importantly, the kinematic wave does not attenuate as it travels downstream. It maintains a constant shape and height. The celerity, U, of the kinematic wave is given by the Kleitz-Seddon equation [*Chanson*, 2004, equation (17.28)],

$$U = \frac{\partial Q}{\partial A}. \tag{16}$$

Assuming a rectangular channel, using equation (15), and employing the relation $V = Q/A$ results in

$$U \sim \frac{3}{2} V. \tag{17}$$

[21] For the diffusion wave approximation, we keep an additional term from equation (11), allowing the free surface and the channel bottom to be nonparallel, resulting in

$$\frac{\partial d}{\partial x} + S_f - S_0 = 0. \tag{18}$$

Assuming a rectangular channel cross section, differentiating the diffusion wave equation (18) and the continuity equation (12), and rearranging results in an advection-diffusion equation (see *Chanson* [2004, pp. 341–342] for a detailed derivation)

$$\frac{\partial Q}{\partial t} + U\frac{\partial Q}{\partial x} = D_t \frac{\partial^2 Q}{\partial x^2}, \tag{19}$$

where

$$U = \frac{3}{2} V\left(1 - \frac{2}{3}\frac{A}{wP_w}\right) \tag{20}$$

is the diffusion wave celerity, with w representing the width of the channel and P_w the wetted perimeter. This celerity is comparable to the kinematic wave celerity, with a small correction factor. In the limit of wide channels (large w) the two celerities converge. The diffusion coefficient is given by

$$D_t = \frac{Q}{2wS_f}. \tag{21}$$

The important difference between the kinematic and the diffusion wave approximations is that the diffusion wave attenuates as it propagates down the channel. Analysis of the range of validity of each of these approximations can be found in the work by *Ponce and Simons* [1977] and *Ferrick* [1985].

[22] Since open channels have intrinsic wave velocities (celerities) we can derive a characteristic response time,

$$\tau_{open} = \frac{L}{U}, \tag{22}$$

where L is the length of the channel. The response time is slightly shorter than, but comparable to, the flow through time of water molecules. It should be noted that unlike in the full pipe case, a partially filled pipe has a response time that would often be comparable to the duration of a recharge event.

3.3. Reservoir/Constriction Systems

[23] The response of a reservoir drained by a pipe-full conduit is determined by both the geometry of the reservoir and the geometry of the conduit that drains the reservoir (Figure 2c). The flow through the system is governed by the Euler equation (1) for flow in a pipe. However, unlike the full pipe case, we assume that the water has different velocities in different parts of the system. Specifically, in the reservoir the velocity will be approximately zero, whereas there can be a significant velocity inside the pipe draining the reservoir. Expanding the total derivative in equation (1), and making the same variable substitutions as for the full pipe case results in

$$\frac{1}{g}\frac{\partial V}{\partial t} + \frac{\partial}{\partial x}\left(h + \frac{V^2}{2g}\right) + \frac{f}{D_H}\frac{V|V|}{2g} = 0. \tag{23}$$

Integrating over the length of the pipe while setting the downstream hydraulic head and the upstream velocity to zero, converting V into Q using the cross-sectional conduit area, and setting the $\partial V/\partial t$ term to zero produces a form of the Darcy-Weisbach equation for slowly varied flow that includes the kinetic energy (or velocity head) effect of acceleration of the fluid from the reservoir into the pipe,

$$Q(t) = A_c\sqrt{\frac{2g}{(1 + fL/D_H)}h(t)}, \tag{24}$$

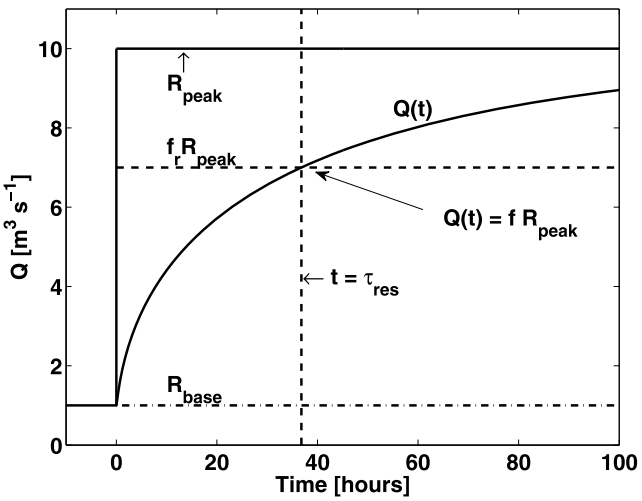

Figure 3. Graph of discharge against time for the reservoir/constriction system based on equation (27) with a square wave recharge function. The horizontal and vertical dashed lines depict the flux value, $f\ R_{peak}$, and the characteristic system time, τ_{res}. The particular discharge curve depicted is calculated by numerically integrating equation (27) for an example case.

where L is the conduit length, $h(t)$ is the height of water above the reservoir bottom as a function of time, and A_c is the cross-sectional area of the conduit (Figure 2c). The continuity equation for the reservoir is

$$\frac{dh}{dt} = \frac{R(t) - Q(t)}{A_R}, \tag{25}$$

where A_R is the surface area (i.e., footprint) of the reservoir, and $R(t)$ is the recharge into the reservoir in units of volume per time. For the purpose of this calculation we assume that the surface area is constant with reservoir depth, h. For simplicity, we define $C_f = 1 + fL/D_H$. Using this definition, substituting equation (24) into equation (25), and separating variables, results in

$$dt = \frac{C_f A_R}{A_c^2 g}\frac{QdQ}{R - Q}. \tag{26}$$

[24] In order to derive the characteristic time of the system, we assume that the reservoir starts from a base flow equilibrium state at time $t = 0$ with $R(0) = Q(0) = R_{base}$. Then the system is perturbed by an instantaneous increase of the input to a value of R_{peak}. The characteristic time can be derived by calculating the time over which the system approaches the new equilibrium. Letting $R(t)$ = constant = R_{peak} and integrating equation (26) from R_{base} to $Q(t)$, we obtain

$$t = \frac{C_f A_R}{A_c^2 g}\left[R_{base} - Q(t) - R_{peak}\ln\left(\frac{R_{peak} - Q(t)}{R_{peak} - R_{base}}\right)\right]. \tag{27}$$

[25] The solution of this equation is shown for an example case in Figure 3. As in the full pipe case, the flow approaches the new equilibrium, R_{peak}, as $t \to \infty$. Thus we let $Q(t) = f_r R_{peak}$, where f_r is some arbitrary value close to one. Furthermore, we define the ratio $R_{ratio} = R_{base}/R_{peak}$. The logarithmic term in equation (27) can then be expressed as

$$\ln\left(\frac{1 - f_r}{1 - R_{ratio}}\right) = \ln(1 - f_r) - \ln(1 - R_{ratio}). \tag{28}$$

Since $f_r \le 1$ and $R_{ratio} \le 1$, we can expand each of these terms in a Maclaurin series (i.e., a Taylor series about $f_r = 0$ and $R_{ratio} = 0$). If we only keep terms up to order two, then equation (27) simplifies to

$$t = \frac{A_R C_f R_{peak}}{2gA_c^2}\left(f_r^2 - R_{ratio}^2\right). \tag{29}$$

By definition $f_r^2 \sim 1$. Since 1) karstic aquifers are known to be flashy, i.e., $Q_{peak} \gg Q_{base}$ [*White*, 1988], 2) we are concerned only with flood events, and 3) a small number squared is even smaller, we let $R_{ratio}^2 \sim 0$. With these approximations the reservoir response time is

$$\tau_{res} \sim \frac{A_R C_f R_{peak}}{2gA_c^2}. \tag{30}$$

Note, that the reservoir response time is a function of the peak recharge as well as the geometry of the reservoir and the constriction.

3.4. Matrix

[26] By our definition, flow through the matrix portion of a karstic aquifer is laminar. We classify fractures large enough to carry turbulent flow as conduits, and those carrying laminar flow as part of the matrix. The matrix component can have two different effects. First, recharge can occur directly into the matrix and then eventually make its way into the conduit network and flow out of the spring. Second, during a flood event, water can be forced out of high pressure conduits and into the surrounding matrix. This water then ultimately drains back into the conduits after the flood pulse subsides.

[27] With regard to recharge directly into a porous matrix, *Manga* [1999] derives three different characteristic timescales for springs: a hydraulic timescale, a time lag, and a residence time. The first two of these timescales are potentially relevant to the problem of matrix hydrograph response to stormflow, whereas the third is only relevant when considering chemical and thermal evolution of the water in the system.

[28] The shortest of these timescales is the time lag, the time between peak recharge and peak discharge. Assuming that the matrix component is initially filled with water, this time is equal to the time that it takes for the pressure wave to diffuse through the pore space. For a discussion of pressure wave diffusion in Darcian aquifers, see *Saar and Manga* [2003]. However, since this timescale is typically much shorter than the hydraulic timescale, and since we are interested in the limiting timescale, we move on to discuss the hydraulic time scale.

[29] The hydraulic timescale is derived by *Manga* [1999] using hydraulic diffusivity and by *Gelhar and Wilson* [1974] in the approximation of a linear reservoir where

the discharge is proportional to the reservoir volume. For both cases

$$\tau_{\text{hydraulic}} \sim \frac{\phi L^2}{Kd}, \tag{31}$$

where ϕ is the effective porosity, L is the aquifer length scale, K is the hydraulic conductivity, and d is the aquifer depth. Linear reservoir theory has long been used in the study of global karstic aquifer response [*Maillet*, 1905]. *Kovács et al.* [2005] derive a solution similar to the above result in terms of the recession coefficient, $\alpha = 1/\tau_{\text{hydraulic}}$.

3.5. Recharge Events

[30] There are a number of ways in which one could define the timescale of a recharge event or input hydrograph. In this work we will use Gaussian input functions,

$$R_{\text{pulse}}(t) = R_{\text{peak}} \exp\left[-\frac{\left(t - t_{\text{peak}}\right)^2}{2\sigma^2}\right], \tag{32}$$

with a width, σ, and we define the recharge timescale as

$$\tau_{\text{rech}} = \sigma. \tag{33}$$

However, we note that complex recharge events containing a series of peaks, or where dR/dt changes abruptly with time, might not be well characterized by using a discrete event duration as the timescale. In order to map the storm pulse flow onto the base flow we let $R(t) = R_{\text{pulse}}$ when $R_{\text{pulse}} > R_{\text{base}}$ and $R(t) = R_{\text{base}}$ when $R_{\text{pulse}} < R_{\text{base}}$.

4. Characterization of System Response to Transient Flow Using a Dimensionless Number, γ

[31] In the following, we provide a dimensionless number that characterizes the relative importance of element geometry and recharge in determining the storm pulse hydrograph output from the system.

4.1. Method

[32] Given the element characteristic response time and recharge time derived in Section 3, it is possible to calculate a dimensionless number,

$$\gamma = \tau_{\text{element}}/\tau_{\text{rech}}, \tag{34}$$

that characterizes the response of a given aquifer to a given recharge event. The value of γ for a particular element/recharge pair determines whether the pair is in the recharge- or geometry-dominated response regime. In the recharge-dominated regime the output hydrograph shape will be nearly identical to the input hydrograph shape, whereas in the geometry-dominated regime the system will significantly modify the input hydrograph.

[33] In order to explore the parameter space of element geometries and recharges, we run large sets of simulations that randomly sample the parameter space. We simulate full pipe and reservoir cases by integrating their respective governing equations numerically using the Dormand-Prince method, an explicit adaptive step size Runga-Kutta (4,5) algorithm [*Dormand and Prince*, 1980].

[34] Solution of the Saint Venant equations is more complex, and for this task we use the Storm Water Management Model (SWMM) developed by the U.S. Environmental Protection Agency [*Rossman*, 2005]. SWMM, designed to simulate urban storm water drainage, is an excellent match to our conceptual model of a karstic aquifer. The code contains pipe elements that can be filled or partially filled, reservoirs with arbitrary geometries, and even has the capability to calculate exchange with a surrounding Darcian aquifer analogous to the porous matrix of karst. In this work, we only use SWMM to calculate flow through open channel systems. SWMM uses the full dynamical solution of the Saint Venant equations (11) and (12), allowing for accurate simulation of storm pulses moving through the system (see *Rossman* [2005, 2006] for details). We have constructed an interface for SWMM that allows one to quickly run large sets of simulations of conduit networks with various geometries and input hydrographs.

[35] For this study, we only simulate flow through simple "single-element" systems. This allows us to examine a range of element parameters and recharges in order to test and validate the analysis in Section 3 and to determine critical values of γ indicating the transition in system responses from recharge- to geometry-dominated regimes.

[36] In order to quantify the system response, we calculate the normalized cross correlation between the input hydrograph and the output hydrograph,

$$\hat{R}_{\text{R,Q}}(t) = \frac{\int_{-\infty}^{\infty} R\left(t + t'\right) Q\left(t'\right) dt'}{\sqrt{\left(\int_{-\infty}^{\infty} R(t)R(t')dt'\right)\left(\int_{-\infty}^{\infty} Q(t)Q(t')dt'\right)}}. \tag{35}$$

This provides a quantitative measure for the similarity of the shape of the input and output hydrographs. If the recharge and discharge have the same shape then the peak of the cross-correlation function, $\text{Max}(\hat{R}_{\text{R,Q}}) = \hat{R}_{\text{R,Q}}(t_{\text{lag}})$, which is at $t = t_{\text{lag}}$, will have a value of one. For cases where the recharge and discharge have different shapes, the peak of the cross correlation will be less than one.

[37] This approach works for both the open channel and reservoir cases. However, the full pipe, by definition, has $R(t) = Q(t)$, and thus the cross correlation of these two functions always results in a value of one. Therefore, in order to characterize the response of the full pipe, we compute the cross correlation of the output flow rate calculated including the momentum response, with the flow rate that the conduit would have if it responded instantaneously to the changing pressure gradient. These curves are shown for an example case in Figure 4. This approach allows us to quantify the effect of the momentum response time (equation (10)).

[38] Since system responses smoothly grade from recharge to geometry dominated, choice of a critical γ value for this transition is somewhat arbitrary. However, the relations between γ and cross correlation for these systems all contain 'knees,' above and below which the function can be approximated roughly as a power law, where the power laws above and below the knee have two different slopes. In order to reduce the arbitrariness of the choice of a critical value of γ, we chose critical values for each system at the

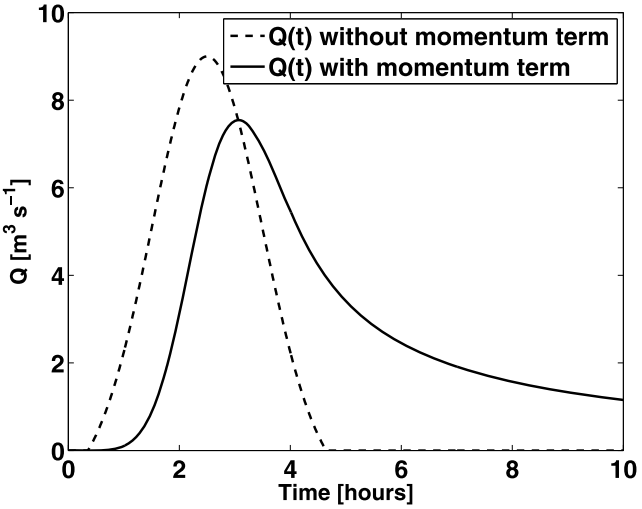

Figure 4. Hydrographs shown for the full pipe case including the momentum response (solid) and neglecting it (dashed). The cross correlation of these two curves provides a means of quantifying the effect of momentum on the response of the system to a changing hydraulic head gradient.

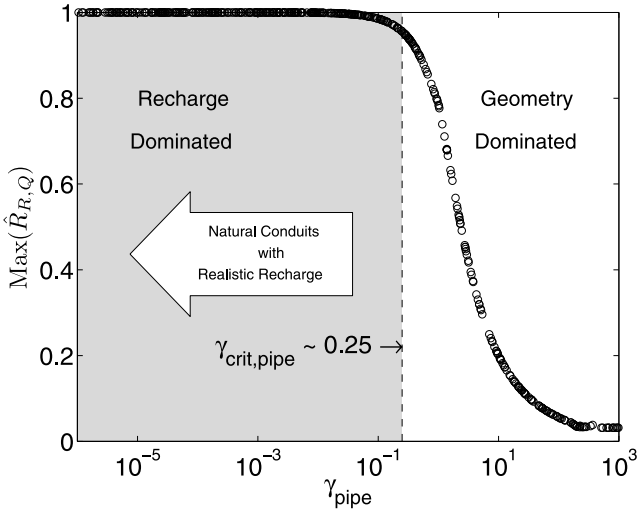

Figure 5. Full Pipe Response. The maximum of the cross correlation function, $\mathrm{Max}(\hat{R}_{R,Q})$, as a function of the dimensionless number, $\gamma_{\mathrm{pipe}} = \tau_{\mathrm{mom}}/\tau_{\mathrm{rech}}$. The circles depict 500 simulations with conduit diameter, Darcy friction factor, recharge peak, and recharge duration chosen at random from a uniform distribution in log space with minimum and maximum values listed in Table 1. The aquifer response can be divided into two regimes: a recharge-dominated regime at low γ and a geometry-dominated regime at high γ. The critical value that differentiates these regimes for a full pipe is $\gamma_{\mathrm{crit,full}} \sim 0.25$. For almost all natural karst conduits and realistic input hydrographs $\gamma_{\mathrm{pipe}} \ll 0.25$.

knee in the relation. This also roughly corresponds to the γ value above which the hydrograph is visibly modified by the system.

4.2. Full Pipe Response

[39] Since the momentum response time is much greater than the pressure wave response time for a full pipe, we calculate the dimensionless ratio of pipe response time to recharge time as

$$\gamma_{\mathrm{pipe}} = \frac{\tau_{\mathrm{mom}}}{\tau_{\mathrm{rech}}} = \frac{D_{\mathrm{H}}}{\sigma F V_{\mathrm{f}}}, \tag{36}$$

where σ is the width of the recharge Gaussian. We simulate 500 randomly selected cases with pipe parameters chosen uniformly in log parameter space with values in the ranges given in Table 1. The four parameters that affect the pipe response are diameter, Darcy-Weisbach friction factor, recharge peak, and recharge duration. The downstream head is set to zero and the upstream head as a function of time is set to the value that would produce a Gaussian hydrograph with a peak, R_{peak}, and a width σ in the slowly varying flow regime in which momentum can be neglected and the Darcy-Weisbach equation (6) is valid.

[40] The maximum value of the cross correlation between the simulated hydrograph, calculated from equation (5), and the hydrograph calculated from the Darcy-Weisbach equation is plotted against γ_{pipe} in Figure 5. There is a tight relation between system response and γ, with a critical value around $\gamma_{\mathrm{crit,pipe}} = 0.25$. If γ is smaller than this critical value then the momentum response is fast enough that it has no significant effect on the hydrograph. However, if γ is greater than this critical value then the pipe response can affect the hydrograph. For natural karstic aquifers almost all cases lie in the low-γ region such that momentum response is unimportant. In order to fill out the curve in Figure 5 the simulation set includes somewhat unrealistic cases with very short recharge durations (as short as 30 s), and very large diameters (as large as 50 meters). It is only for these rare cases that one would expect momentum in full pipe flow to be important. However, if there are any sharp, or high frequency, features in the input hydrograph this momentum effect will wash them out with a cutoff frequency of roughly $1/\tau_{\mathrm{mom}}$.

Table 1. Ranges From Which Parameter Sets Were Uniformly Drawn in Log Space in Order to Calculate the Relationship Between γ_{pipe} and $\mathrm{Max}(\hat{R}_{R,Q})$ for Full Pipes

	Minimum	Maximum	Units
D_{H}	0.1	50	m
F	0.01	0.1	unitless
R_{peak}	0.5	50	m^3/s
σ	0.0083 (30 s)	12.0	h

Table 2. Ranges From Which Parameter Sets Were Uniformly Drawn in Log Space in Order to Calculate the Relationship Between γ_{open} and $\mathrm{Max}(\hat{R}_{R,Q})$ for Open Channel Flow

	Minimum	Maximum	Units
L	1,000	30,000	m
D_{H}	1	20	m
f	0.01	0.1	unitless
S_0	0.001	0.02	unitless
R_{base}	0.1	1.0	m^3/s
R_{peak}	0.2	20	m^3/s
σ	0.5	12.0	h

4.3. Open Channel Response

[41] Note that τ_{open} was derived using the wave celerity. Furthermore, the celerity of kinematic waves and diffusion waves were slightly different. However, we find that the kinematic wave celerity (equation (17)) is sufficiently accurate for our purposes, particularly when the channel depth is small compared to the width. Therefore, we calculate

$$\gamma_{open} = \frac{\tau_{open}}{\tau_{rech}} = \frac{2L}{3V\sigma}, \tag{37}$$

where we chose $V = V_{peak}$ to be the equilibrium velocity for an input $R = R_{peak}$. V_{peak} is computed by calculating the depth of the flow via equation (15). For the wide channel limit the equation can be solved analytically, otherwise the depth can be calculated iteratively.

[42] There are four geometrical parameters that affect the response of an open channel to transient flow: 1) length, 2) diameter, 3) roughness, and 4) slope. Additionally the recharge peak, and duration can affect the aquifer response. In order to characterize the relationship between γ_{open} and aquifer response, we plot γ_{open} against $\mathrm{Max}(R_{R,Q})$ for 500 simulations using randomly chosen parameter sets. These parameters were chosen from a uniform distribution in log space between the maximum and minimum values noted in Table 2. After random selection, parameter sets are filtered to assure that no cases are included where the flow is large enough that the conduit transitions from open channel to full pipe flow during the course of the simulation. If a parameter set falls within this transitional range then it is replaced with another random selection.

[43] The open channel response as a function of γ is shown in Figure 6. The similarity of the input and output hydrographs, characterized by the maximum of the cross correlation, varies smoothly as a function of γ. For very low γ, the input and output hydrographs look nearly identical, whereas for high γ the output hydrograph has been significantly modified by the system. The critical value of γ that separates the recharge- and geometry-dominated regimes for the open channel is $\gamma_{crit,open} \sim 5$. The recharge-dominated regime is also equivalent to the portion of the parameter space where the kinematic wave equation is a good approximation, because the kinematic wave does not change shape as it propagates down the channel.

[44] In order to illustrate the storm pulse propagation down open channels in real karstic aquifers, we chose two example cases of karstic systems with significant open channel portions. Our first example case is Krina jama in Slovenia [*Prelovšek et al.*, 2008] (Figures 6a and 6b). Though parts of the system are unknown, a large portion of the system functions as an open channel. Given the description by *Prelovšek et al.* [2008] we approximate the open channel portion of the system with $L = 3000$ m, $w = 5$ m, and $S_0 = 0.02$. We simulate two storms, each with a base recharge of $R_{base} = 1\ m^3s^{-1}$ and a peak recharge of $R_{peak} = 10\ m^3s^{-1}$. The first storm, depicted in Figure 6a, has $\sigma = 24$ h, and the second storm, depicted in Figure 6b has $\sigma = 0.5$ h. γ_{open} for both of these storms falls well within the recharge-dominated regime. As shown by comparison of the input and output hydrographs, the system produces very little modification to the shape of the storm hydrograph.

[45] The second example case is Buckeye Creek Cave in West Virginia, which has been the subject of a number of hydrology and geomorphology studies [*Springer and Wohl*, 2002; *Springer et al.*, 2003; *Springer*, 2004]. In low flow conditions, this system is an open channel conduit along its entire length. Drawing parameters from the studies above we approximate the system with $L = 1750$ m, $w = 10$ m, and $S_0 = 0.01$. Both example simulations are run with $R_{base} = 0.5\ m^3s^{-1}$ and $R_{peak} = 5\ m^3s^{-1}$. Again we use values of $\sigma = 24$ h and $\sigma = 0.5$ h, shown in Figures 6c and 6d, respectively. For this system the simulations also remain in the recharge-dominated regime, even for the extreme case of a 0.5 hour storm pulse. However, the extreme case is approaching the critical value of γ_{open}, and there is some modification of the shape of the pulse shown in Figure 6d.

[46] As can been seen from the distribution of random cases in Figure 6, and our two example cases, the response of most open channels in karstic aquifers will be recharge dominated. Only long channels, combined with short pulses will produce significant modifications. One caveat here, is that we are assuming a uniform open channel. It is quite possible that open channels with cross sections that drastically change along their length will produce modifications. However, study of irregular channels is beyond the scope of this work.

4.4. Reservoir/Constriction Response

[47] The dimensionless number characterizing reservoir response is

$$\gamma_{res} = \frac{\tau_{res}}{\tau_{rech}} = \frac{A_R C_f R_{peak}}{2gA_c^2\sigma}, \tag{38}$$

and therefore the response is a function of constriction length, diameter, and roughness as well as the reservoir surface area, the peak recharge, and the storm duration. As for the open channel case, we simulate output hydrographs by randomly selecting reservoir/constriction properties from a uniform distribution in log space. The maximum and minimum parameter values are listed in Table 3.

[48] For systems with $\gamma_{res} \gtrsim 1$ the geometry of the aquifer strongly affects the output hydrograph (Figure 7). For systems with γ_{res} below this critical value the shape of the output hydrograph is controlled by the shape of the recharge hydrograph. We define the boundary between the input-dominated regime and the geometry-dominated regime as $\gamma_{crit,res} = 1$.

[49] We chose two example cases of real karstic aquifers in order to demonstrate the effects of different system geometries and recharge hydrographs. One system that can be represented as a single reservoir/constriction at higher flow levels is the Devil's Icebox in Missouri [*Halihan and Wicks*, 1998]. We pull the geometrical parameters from *Halihan and Wicks* [1998], using $D_H = 1.65$ m, $L = 25$ m, $A_R = 4000\ m^2$, and $f = 0.1$. We simulate two different recharge events with the same base flow, $R_{base} = 1.0\ m^3s^{-1}$, and peak flow, $R_{peak} = 10.0\ m^3s^{-1}$, where one event has $\sigma = 24$ h and the other has $\sigma = 1$ h. These simulations are depicted as squares in Figure 7, and the hydrographs are shown in Figures 7a and 7b. For this set of parameters the system does not significantly modify the input hydrograph, though

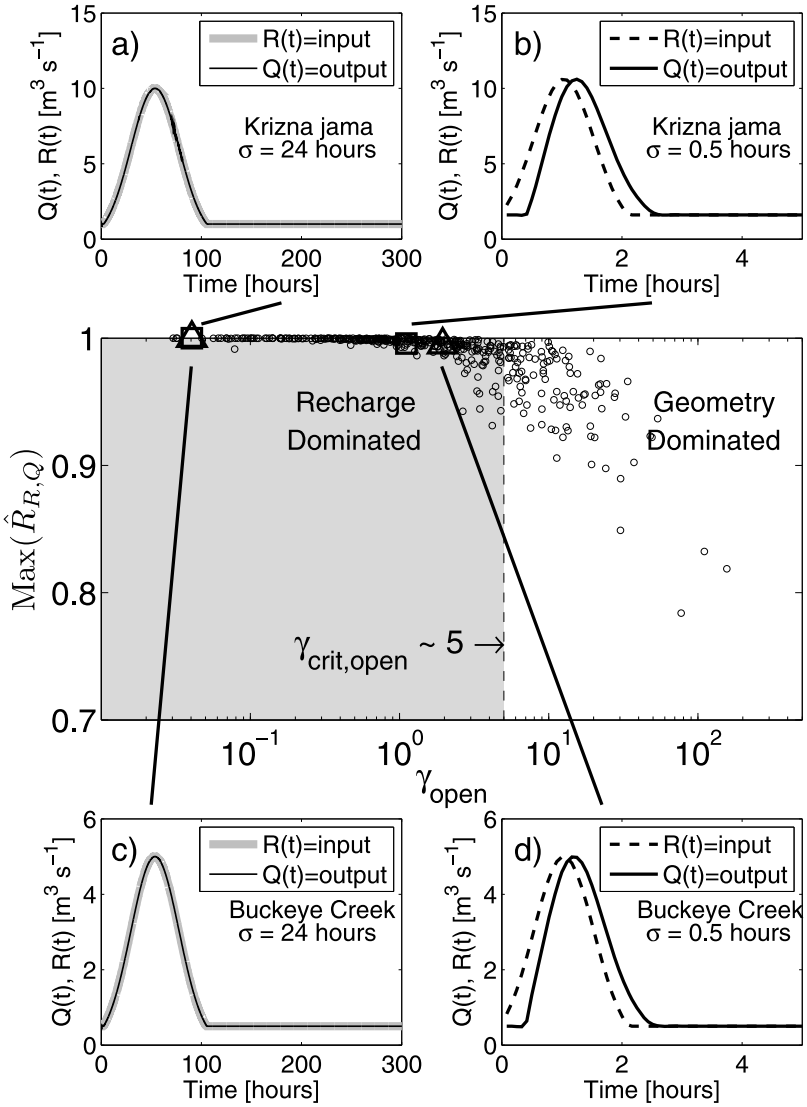

Figure 6. Open Channel Response. The maximum of the cross correlation function, Max($\hat{R}_{R,Q}$), as a function of the dimensionless number $\gamma_{open} = \tau_{open}/\tau_{rech}$. The circles depict 500 simulations with conduit length, diameter, roughness, slope, recharge peak, and recharge duration chosen at random from a uniform distribution in log space with minimum and maximum values listed in Table 2. The aquifer response can be divided into two regimes: a recharge-dominated regime at low γ and a geometry-dominated regime at high γ. The critical value that differentiates these regimes for open channels is $\gamma_{crit,open} \sim 5$. The squares and triangles depict example cases from Krina jama and Buckeye Creek Cave, respectively. (a–d) The hydrographs depict the input and output hydrographs for these systems for two different storms. The storms in Figures 6a and 6c have $\sigma = 24$ h, whereas for Figures 6b and 6d $\sigma = 0.5$ h.

the event with a duration of one hour is approaching the critical value of γ.

[50] The second example system is Škocjanske jame from Slovenia. This system is a string of reservoir/constrictions [*Gabrovšek and Peric*, 2006]. We produce a crude model of one of these constrictions, following *Gabrovšek and Peric* [2006], using $D_H = 2.0$ m, $L = 1000$ m, $A_R = 2000$ m^2, and $f = 0.1$. For this system we run two simulations with the same storm durations as for Devil's Icebox, but with $R_{base} = 5.0$ m^{3}s^{-1} and $R_{peak} = 150$ m^{3}s^{-1}. These simulations are shown in Figure 7 as triangles, and the hydrographs are depicted in Figures 7c and 7d. This system is much more likely to modify the shape of the storm pulse than the previous example. For the 24 hour storm the system lies in

Table 3. Ranges From Which Parameter Sets Were Uniformly Drawn in Log Space in Order to Calculate the Relationship Between γ_{res} and Max($\hat{R}_{R,Q}$) for Reservoir/Constriction Systems

	Minimum	Maximum	Units
L	10	50	m
D_H	0.1	1.0	m
f	0.01	0.1	unitless
A_R	100	10,000	m^2
R_{base}	0.01	10	m^3/s
R_{peak}	0.02	500	m^3/s
σ	0.5	30	h

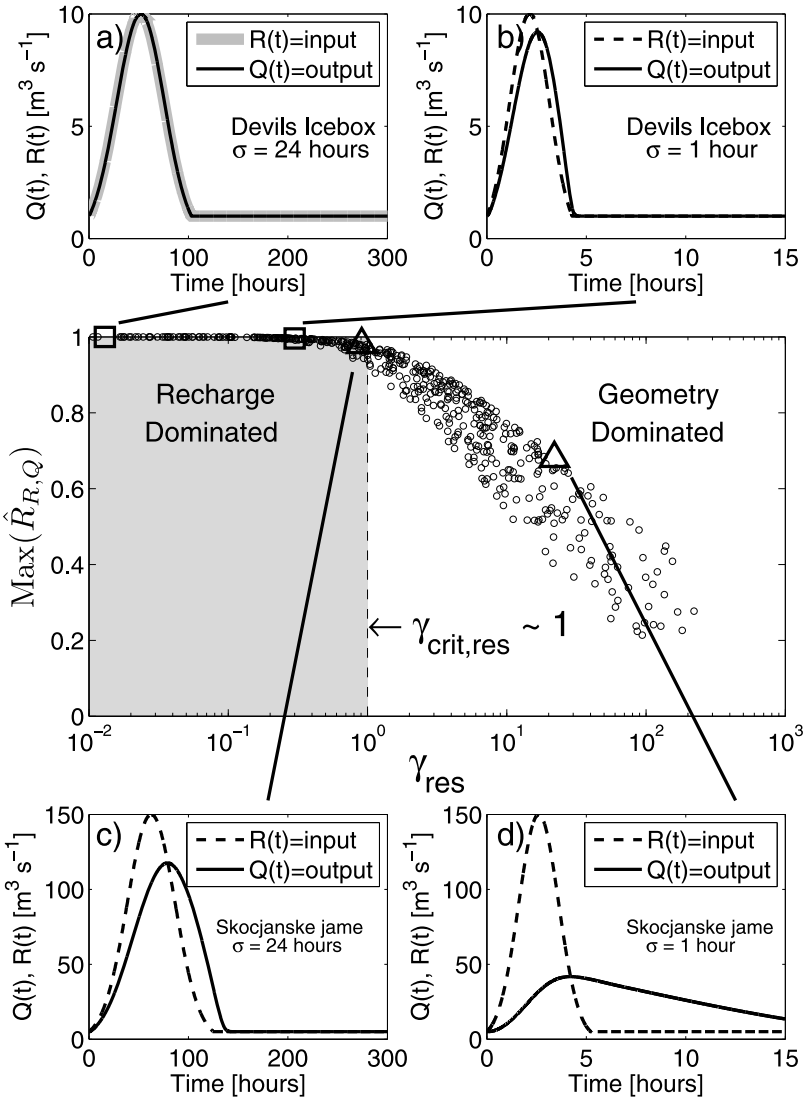

Figure 7. Reservoir/Constriction Response. The maximum of the cross correlation function, $\mathrm{Max}(\hat{R}_{R,Q})$, as a function of the dimensionless number $\gamma_{res} = \tau_{res}/\tau_{rech}$. The circles depict 500 simulations with constriction length, diameter, roughness, and reservoir surface area and recharge peak and duration chosen at random from a uniform distribution in log space with minimum and maximum values listed in Table 3. The aquifer response can be divided into two regimes: a recharge-dominated regime at low γ and a geometry-dominated regime at high γ. The critical value that differentiates these regimes for reservoir/constriction elements is $\gamma_{crit,res} \sim 1$. The squares and triangles depict example cases from Devil's Icebox and Škocjanske jama, respectively. (a–d) The hydrographs depict the input and output hydrographs for these systems for two different storms. The storms in Figures 7a and 7c have σ = 24 h, whereas for Figures 7b and 7d σ = 1 h.

the transition zone near the critical value of γ, whereas the 1 hour pulse is far into the geometry-dominated regime. These results agree with the data from *Gabrovšek and Peric* [2006], which show significant modification of flood pulses as the pulses travel through the cave restrictions.

4.5. Matrix Response

[51] The matrix timescale is typically much longer than that of a storm event, and thus

$$\gamma_{matrix} = \frac{\tau_{matrix}}{\tau_{rech}} \tag{39}$$

is typically large. For example, using length scales and parameters appropriate for even a small karstic basin, with L = 1000 m, d = 10 m, ϕ = 0.01, and $K = 10^{-4}$ m s^{-1} results in $\tau_{hydraulic}$ = 116 days. However, one must also remember that real karst basins are often broken up into smaller matrix blocks that are separated by conduits. These smaller matrix blocks can have response times that are much shorter. For example, reducing the characteristic length scale to L = 100 m results in $\tau_{hydraulic}$ = 1 day. *Kovács et al.* [2005] studied two-dimensional networks of conduits and matrix, with each matrix block draining to the conduits that surround it. They demonstrate that once recharge has ended the spring recession hydrograph is primarily determined by

the nature of the porous matrix blocks. This is because the characteristic time of the matrix blocks is typically much larger than that of the conduits. *Hergarten and Birk* [2007] extend this result to the case of fractal distributions of matrix block sizes and demonstrate that the smaller blocks, which have shorter characteristic times, determine the early response, whereas the larger blocks, with longer characteristic times, determine the long-term response.

[52] *Geyer et al.* [2008] specifically study the relation between recharge and discharge from a karstic aquifer using a dual-permeability linear reservoir model. The high-permeability reservoir represents the conduits, whereas the low-permeability reservoir represents the porous matrix. They show that if there is a significant proportion of recharge into the matrix component then the discharge does not resemble the recharge. Rather, they find that the first derivative of the spring hydrograph roughly resembles the recharge. Since the matrix has a response time typically much longer than the duration of storms, a storm hydrograph input into the matrix, rather than directly into the conduits, will in most cases be significantly modified by the matrix. That is, the discharge hydrograph from the matrix component will not resemble the recharge hydrograph into it.

[53] Additionally, in most cases, exchange between the matrix and conduits is not likely to contribute significantly to storm response, since the time required for significant flow into the matrix is longer than the typical storm duration. Using numerical simulations, *Peterson and Wicks* [2005] showed that for a variety of parameters the exchange flow between a conduit and the porous medium surrounding it was insignificant compared to the total stormflow. While there are likely exceptions to this rule, in the remainder of this work we neglect the effect of water exchange between matrix and conduits on storm response.

[54] The significantly different response timescales of the conduit flow and matrix flow may allow separation of spring hydrographs into the early portion that is governed by conduit response and late portion that is due to delayed matrix flow. In fact, standard base flow recession analysis of stream hydrographs relies on this delayed response of standard groundwater flow through porous media to distinguish between the groundwater (base flow) portion and other water sources to the stream hydrograph. It is also common practice to similarly separate spring flows from karstic systems [*Dreiss*, 1982]. However, while the matrix response in many cases will be separable, for some cases it may be difficult or impossible to distinguish the internal matrix drainage component from the recession of a stream input. This particularly holds for systems where recharge into the system is dominantly from surface streams that sink at the boundary of the karstic aquifer. Additionally, systems with very small porous matrix blocks may have response timescales short enough to affect the early portions of recession [*Hergarten and Birk*, 2007].

[55] Since our equations (10), (22), (30), and (31) provide characteristic timescales for full-pipe, open channel, reservoir/constriction, and matrix flow, respectively, for a system with known geometry we can estimate the time after the peak spring discharge when the spring hydrograph should no longer be used for the analysis presented in this paper. As the characteristic timescale for flow in the rock matrix is being reached, neglecting the matrix component is no longer valid. Conversely, the same matrix characteristic time can serve as a temporal starting point beyond which the spring hydrograph time series becomes useful for studies concerned with porous medium flow within the rock matrix.

4.6. Scatter in the γ–Cross Correlation Plots

[56] The three plots of γ versus the input-output cross correlation show a range of scatter. Specifically, the plot for the full pipe cases (Figure 5) shows essentially no scatter, whereas the reservoir/constriction plot shows an intermediate amount of scatter (Figure 7), and the open channel plot (Figure 6) shows the largest amount of scatter. This variation in scatter largely results from the varying degrees of approximation needed in order to calculate the characteristic system response times, with the full pipe requiring no approximation, and the reservoir/constriction and open channel requiring successively more approximation. Additionally, we note that the plot for the full pipe case is fundamentally different from the other two, as it depicts the cross correlation of the full pipe responses with and without the momentum term, whereas the other plots cross correlate input and output. Thus, the full pipe plot only depicts the increasing effect of the single momentum term with shorter storm pulses. This may account for the lack of scatter for the full pipe. In any case, the scatter introduced by these effects is small enough that the general conclusion concerning different response regimes remains sound.

4.7. Time Lags

[57] The cross correlation of input and output hydrographs allows us to quantify the similarity of their shapes, but it also provides us with the value of the time lag between the peak input and peak output. This time lag can be used to obtain information about the system, particularly if combined with the lags in the temperature and conductivity responses [*Birk et al.*, 2004, 2006]. With a careful selection of system parameters one could construct a system with almost any combination of γ and time lag. However, if system parameters are drawn uniformly, as in our study, then there is a positive correlation between γ and the time lag. This makes intuitive sense as the longer a wave remains in the system, the more time and distance it has to be modified by the system. This relation is depicted in Figure 8 for both the open channel and reservoir/constriction cases.

5. Discussion and Conclusions

[58] We demonstrate that ignoring the recharge function could lead to spurious interpretations of spring hydrographs and associated aquifer characteristics. Specifically, we find that different karstic aquifer system elements have inherent response timescales, τ_{element}. Whenever the timescale of a recharge event, τ_{rech}, is much larger than the system timescale then the shape of the output hydrograph matches the shape of the input hydrograph. Conversely, if the timescale of the recharge event is much shorter than the response time of the system then the output hydrograph is modified by the system geometry. A given recharge event and aquifer geometry can be characterized by a dimensionless number, $\gamma = \tau_{\text{element}}/\tau_{\text{rech}}$ and there is a critical value of

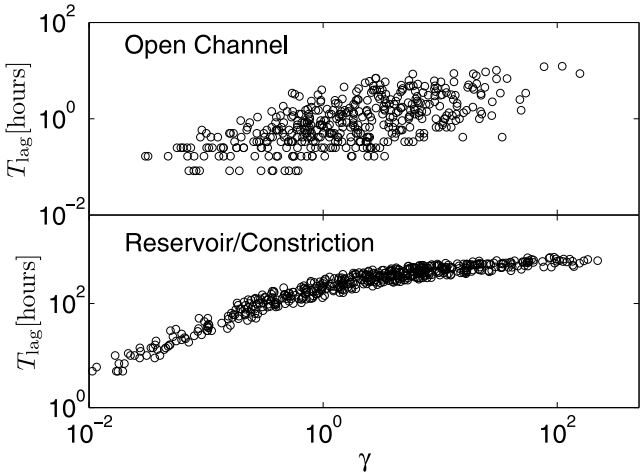

Figure 8. For uniformly chosen system and recharge parameters, γ has a positive correlation with the time lag of the system. This is shown for both (a) the open channel case and (b) the reservoir/constriction case.

γ that divides element/recharge combinations into two types: 1) those for which the response is determined by the recharge and 2) those for which the response is determined by the element geometry. We find that the critical values of γ are $\sim$0.25 for full pipes, $\sim$1 for reservoir/constrictions, and $\sim$5 for open channels.

[59] Recently, *Geyer et al.* [2008] demonstrated a similar result for a phenomenological model of a karstic aquifer. This model approximated a karstic aquifer as a combination of two linear reservoirs, one which was highly permeable (representing the conduit network) and the other which had a low permeability (representing the matrix). For recharge into the high permeability reservoir they find that there are two response regimes. If the recession coefficient of the high permeability reservoir is very large, then the discharge from the aquifer resembles the recharge. If the recession coefficient is very small then the time derivative of the discharge resembles the recharge. These correspond to our recharge-dominated and geometry-dominated responses, respectively.

[60] They further argue that natural karstic aquifers have high enough recession coefficients that they lie in the geometry-dominated regime. While this is true for the linear reservoir model, and for their specific study case, our work demonstrates that this need not hold for all karstic aquifers. Specifically, when one considers the pipe flow and open channel equations for single-element aquifers there are realistic regions of the parameter space where the response will be recharge dominated (low γ). Whether or not a given aquifer is in the recharge-dominated regime will be a function of both aquifer geometry and the recharge function. Additionally, we find that there are realistic regimes where the geometry of the system so heavily modifies the hydrograph that the discharge cannot be used to reconstruct the recharge without information about the geometry, particularly in the reservoir/constriction case. The approach by *Geyer et al.* [2008] was to represent the aquifer globally with a lumped parameter model, whereas in this work we analyze karstic aquifers at the small scale of an individual segment of conduit. More work is needed in order to understand the scaling of aquifer response with network complexity. In which cases are compound networks of elements well approximated by such global lumped parameter models, and in which cases do the global models break down?

[61] Other prior work has examined the recession from two-dimensional conduit networks embedded in a porous matrix through a combination of analytical techniques and numerical simulations [*Kovács et al.*, 2005; *Hergarten and Birk*, 2007]. *Kovács et al.* [2005] divide these conduit/matrix systems into two flow regimes "matrix restrained" and "conduit influenced." In the matrix-restrained flow regime the properties of the matrix blocks determine the recession curve, whereas in the conduit-influenced regime the conduits draining the blocks also have an effect on the recession. They show that mature karstic aquifers typically lie in the matrix-restrained regime, whereas immature karst or fractured aquifers may be conduit influenced. *Hergarten and Birk* [2007] generalize this work to aquifers with a distribution of matrix block sizes and show that the size distribution of the smallest blocks determines the early recession, whereas the size of the largest blocks determines the long-term recession.

[62] These studies have two notable limitations. First, rather than considering changing boundary conditions, as resulting from a storm, they assume an initial state where the matrix and conduits are full and drain over time. Thus, the analysis may not hold for sufficiently brief storms, as noted by *Hergarten and Birk* [2007]. Second, these models only hold for times after which recharge has ceased.

[63] In general, the results found in these prior studies of matrix/conduit networks can be cast within the framework of the current study. In the matrix-dominated regime of *Kovács et al.* [2005] the characteristic timescale of the conduit network is much less than that of the matrix. On the contrary, in the conduit-influenced regime the characteristic time of the conduit network is long enough that the matrix and conduit responses both contribute to the recession. Their conclusion that most karstic aquifers are matrix-dominated concords with our finding that the matrix timescale is typically significantly longer than the conduit timescale. However, the current study also provides a means for going beyond the noted limitations of the previous study. Specifically, our model applies for times when the recharge is still occurring and for storms with an arbitrary duration. We show that in some realistic configurations mature conduit networks can influence the discharge hydrographs, particularly for brief storms or systems with constrictions. We also provide a method for determining the effect that the changing recharge may have on the discharge hydrograph. The primary limitation of our model is that it is currently only applied to single karst network elements.

[64] However, some real karstic aquifers are well approximated as single element systems. For example, in lower flow regimes, Buckeye Creek Cave is essentially a 1.75 km long open channel. During high flow, the response of Devil's Icebox is well fit by a single reservoir/constriction model [*Halihan and Wicks*, 1998]. However, the majority of karstic aquifers are complex networks of many elements, combined in series and parallel. It is not yet clear how the characteristic times of compound networks of elements, as

used in the two-dimensional matrix/conduit models discussed above, will differ from the characteristic times of single element systems. Additionally most karstic aquifers have portions that undergo transitions from one element type to another once a critical flow stage is reached. An open channel can transition into a full pipe which then backs up water into a reservoir behind it. As water levels change, more flow paths can also become accessible. Therefore, systems can undergo an instantaneous state change from one γ regime into another. Another effect present in complex networks that is not accounted for by our single element model is backflow of tributaries, where the flow of a given path can be momentarily shut down or even reverse. These more complex effects will be the subject of future research.

[65] For realistic single-element aquifers we provide the following general observations: 1) full pipes tend to have the lowest γ values, almost always falling in the recharge-dominated regime, 2) open channels also typically have low γ values and produce little modification of the recharge pulse, 3) reservoir/constrictions can fall in either regime, but often produce significant modifications of the pulse, and 4) matrix elements always produce a significant modification of the recharge hydrograph. It is also worth noting that while open channels and reservoir/constrictions may occur in isolation, it is rare to have a full pipe that is not connected to some sort of reservoir upstream, be it a surface sinkhole, a larger open channel section, or a cavernous void. In order to not have a reservoir upstream, the entry to a full pipe segment must have an easily accessible overflow route, such that the overflow immediately takes all recharge that exceeds the pipe's capacity.

[66] Here we derive discrete timescales for both aquifer elements and recharge events. However, this approach may fail in the case of complex recharge functions. Specifically, we note that whether or not an input signal is modified is partially dependent on the time derivative of the input hydrograph. Regions with sharp features in the hydrograph are blurred out, whereas regions where the recharge is changing very slowly over time produce little modification of the input hydrograph. This is particularly important for the case of recession curves. If the input into the system undergoes a slow recession, as most surface streams do, then one would expect to see a similar recession at the output. Often the recession curves at karst springs are used to estimate aquifer properties. This approach is faulty in the case of receding inputs, as the recession will be a superposition of both the receding input and internal matrix drainage. While this work has focused on discrete events, it is likely possible to develop a parallel analysis that provides a quantity analogous to γ that is a continuous function of time over a recharge event. Exploration of a continuous characterization of response is left for future work.

[67] While the bulk of our discussion has focused on understanding the responses of karstic aquifers to storms, this work also applies to glacial hydrology. Glaciers are often drained by networks of conduits [*Fountain and Walder*, 1998]. As for many karstic aquifers, the conduits are typically inaccessible. The conduit system can control basal pressures and therefore is important in determining sliding and melting rates [*Willis*, 1995; *Fountain and Walder*, 1998]. A number of studies have analyzed hydrographs and tracer breakthrough curves at conduits exiting glacier snouts in order to derive information about the evolution of the drainage system over a melt season [*Nienow et al.*, 1996, 1998; *Swift et al.*, 2005; *Willis et al.*, 2009]. Since the equations governing the flow through glacial conduits are the same as those for karst conduits, the work here also applies to these systems. Specifically, in such analysis it is important to consider the form of the recharge into the system, which would be expected to evolve over the season as the snowpack melts away.

[68] We have elucidated the fundamental physics that governs the response of individual elements of karstic aquifers. However, the ultimate pragmatic goal of such analysis is the determination of karstic aquifer properties via observation of aquifer response, an inverse modeling problem. As noted above, significant additional complexity may arise in the compound networks of elements needed to represent most real-world karstic aquifers. However, this complexity aside, we have demonstrated that the functional form of the recharge can present a hurdle to determining aquifer geometry. Namely, if the recharge timescale is much longer than the response timescale of the system then the discharge hydrograph can be nearly identical to the recharge hydrograph. In this case the discharge hydrograph will contain little geometrical information about the system. The inverse problem of determining aquifer properties remains unsolved. However, we provide a framework for determining some potential limitations to the solution of the inverse problem. Specifically, the inverse problem cannot be properly approached until one answers the question: To what extent is the discharge a function of the recharge versus the system geometry? Here we provide an answer to this question that is valid for at least simple karstic aquifers, and can likely be extended to more complex aquifers. When the recharge timescale is much longer than the aquifer response timescale (small γ), then the discharge resembles the recharge. Conversely, when the recharge timescale is much shorter than the aquifer response time (large γ), then the recharge hydrograph is significantly modified by the system geometry, potentially enabling determination of aquifer geometrical properties via analysis of the response.

Notation

α	recession coefficient
ϵ	wall roughness (length)
γ_{element}	dimensionless element response number
γ_{crit}	critical γ value
ρ	density
σ	storm duration
τ_0	wall shear stress
$\tau_{\text{hydraulic}}$	matrix hydraulic timescale
τ_{mom}	full pipe momentum timescale
τ_{open}	open channel timescale
τ_{rech}	recharge timescale
τ_{res}	reservoir/constriction timescale
$A(x, t)$	cross-sectional flow area
A_{c}	constriction cross-sectional area
A_{R}	reservoir surface area
C_{f}	$1 + fL/D_{\text{H}}$
$d(x, t)$	flow depth
D_{H}	hydraulic diameter

D_t	wave diffusion coefficient
f	Darcy-Weisbach friction factor
f_r	fraction of equilibrium flow
g	Earth's gravitational acceleration
h	hydraulic head
Δh	change in hydraulic head
h_{in}	upstream hydraulic head
h_f	final upstream hydraulic head
K	hydraulic conductivity
L	conduit length
$P(x)$	average pressure in cross section
P_w	channel wetted perimeter
$Q(t)$	aquifer element discharge (vol/time)
$Q(x, t)$	flow rate in channel (vol/time)
$R(t)$	aquifer element recharge (vol/time)
R_{base}	base flow recharge
R_{peak}	peak flow recharge
$R_{pulse}(t)$	storm pulse recharge
R_{ratio}	R_{base}/R_{peak}
$\hat{R}_{R,Q}(t)$	cross correlation of R(t) and Q(t)
Re	Reynold's number
S_0	slope of channel bottom
S_f	friction slope
t_{lag}	lag time between R and Q peaks
U	open channel wave celerity
$V(x, t)$	average velocity in cross section
V_f	final pipe flow velocity
$w(x)$	channel width
x	position along pipe
$z(x)$	elevation of full pipe along length

[69] **Acknowledgments.** M.D.C. is supported by the National Science Foundation (NSF) under Earth Sciences Postdoctoral Fellowship 081647. M.O.S. thanks the George and Orpha Gibson endowment for its support of the Hydrogeology and Geofluids Research Group, and also acknowledges support from NSF grant DMS-0724560. We also thank an anonymous reviewer for insightful suggestions that improved our discussion of related work. Jason Gulley and Alison Banwell brought to our attention the relevance of this work for glacial hydrology. Any opinions, findings, and conclusions or recommendations expressed in this material are those of the authors and do not necessarily reflect the views of the NSF.

References

Ashton, K. (1966), The analysis of flow data from karst drainage systems, *Trans. Cave Res. Group G. B.*, *7*, 161–204.

Benson, R., L. Yuhr, and R. Kaufmann (2003), Some considerations for selection and successful application of geophysical methods, paper presented at Third International Conference on Applied Geophysics, Fed. Highway Admin., Orlando, Fla.

Birk, S., R. Liedl, and M. Sauter (2004), Identification of localised recharge and conduit flow by combined analysis of hydraulic and physico-chemical spring responses (Urenbrunnen, SW-Germany), *J. Hydrol.*, *286*, 179–193.

Birk, S., R. Liedl, and M. Sauter (2006), Karst spring responses examined by process-based modeling, *Ground Water*, *44*, 832–836.

Brown, M. C. (1970), Karst hydrology of the lower Maligne Basin, Jasper, Alberta, *Cave Stud.*, *13*, 179–193.

Brown, M. C. (1973), Mass balance and spectral analysis applied to karst hydrologic networks, *Water Resour. Res.*, *9*, 749–752.

Chanson, H. (2004), *The Hydraulics of Open Channel Flow: An Introduction*, 2nd ed., Elsevier, Burlington, Mass.

Denic-Jukic, V., and D. Jukic (2003), Composite transfer functions for karst aquifers, *J. Hydrol.*, *274*, 80–94.

Dormand, J. R., and P. J. Prince (1980), A family of embedded Runge-Kutta formulae, *J. Comput. Appl. Math.*, *6*, 19–26.

Dreiss, S. (1982), Linear kernels for karst aquifers, *Water Resour. Res.*, *18*, 865–876.

Dreiss, S. (1983), Linear unit-response functions as indicators of recharge areas for large karst springs, *J. Hydrol.*, *61*, 31–44.

Eisenlohr, L., M. Bouzelboudjen, L. Kiraly, and Y. Rossier (1997), Numerical versus statistical modeling of natural response of a karst hydrogeological system, *J. Hydrol.*, *202*, 244–262.

Ferrick, M. G. (1985), Analysis of river wave types, *Water Resour. Res.*, *21*, 209–220.

Florea, L. J., and H. L. Vacher (2006), Springflow hydrographs: Eogenetic vs. teleogenetic karst, *Ground Water*, *44*, 352–361.

Fountain, A. G., and J. S. Walder (1998), Water flow through temperate glaciers, *Rev. Geophys.*, *36*, 299–328.

Gabrovšek, F., and B. Peric (2006), Monitoring the flood pulses in the epiphreatic zone of karst aquifers: The case of Reka River system, Karst Plateau, SW Slovenia, *Acta Carsol.*, *35*, 35–46.

Gelhar, L. W., and J. L. Wilson (1974), Ground-water quality modeling, *Ground Water*, *12*, 399–408.

Geyer, T., S. Birk, R. Liedl, and M. Sauter (2008), Quantification of temporal distribution of recharge in karst systems from spring hydrographs, *J. Hydrol.*, *348*, 452–463.

Grasso, D. A., and P.-Y. Jeannin (2002), A global experimental system approach of karst springs hydrographs and chemographs, *Ground Water*, *40*, 608–618.

Grasso, D. A., P.-Y. Jeannin, and F. Zwahlen (2003), A deterministic approach to the coupled analysis of karst springs' hydrographs and chemographs, *J. Hydrol.*, *271*, 65–76.

Halihan, T., and C. M. Wicks (1998), Modeling of storm responses in conduit flow aquifers with reservoirs, *J. Hydrol.*, *208*, 82–91.

Henderson, F. (1963), Flood waves in prismatic channels, *J. Hydraul. Div. Am. Soc. Civ. Eng.*, *89*, 39–67.

Hergarten, S., and S. Birk (2007), A fractal approach to the recession of spring hydrographs, *Geophys. Res. Lett.*, *34*, L11401, doi:10.1029/2007GL030097.

Kaufmann, G. (2009), Modeling karst geomorphology on different timescales, *Geomorphology*, *106*, 62–77.

Kiraly, L., P. Perrochet, and Y. Rossier (1995), Effect of the epikarst on the hydrograph of karst springs: A numerical approach, *Bull. Hydrogeol.*, *14*, 199–220.

Knisel, W. (1972), Response of karst aquifers to recharge, *Hydrol. Pap. 60*, pp. 1–51, Colo. State Univ., Fort Collins.

Kovács, A., P. Perrochet, L. Király, and P.-Y. Jeannin (2005), A quantitative method for the characterisation of karst aquifers based on spring hydrograph analysis, *J. Hydrol.*, *303*, 152–164.

Labat, D., R. Ababou, and A. Mangin (2000a), Rainfall-runoff relations for karstic springs. Part I: Convolution and spectral analyses, *J. Hydrol.*, *238*, 123–148.

Labat, D., R. Ababou, and A. Mangin (2000b), Rainfall-runoff relations for karstic springs. Part II: Continuous wavelet and discrete orthogonal multiresolution analyses, *J. Hydrol.*, *238*, 149–178.

Larock, B. E., R. W. Jeppson, and G. Z. Watters (2000), *Hydraulics of Pipeline Systems*, CRC Press, Boca Raton, Fla.

Maillet, E. (1905), *Essais d'Hydraulique Souterraine et Fluviale*, Hermann, Paris.

Manga, M. (1999), On the timescales characterizing groundwater discharge at springs, *J. Hydrol.*, *219*, 56–69.

Milanovic, P. T. (1976), Water regime in deep karst: Case study of the Ombla Spring drainage area, in *Karst Hydrology and Water Resources*, vol. 1, edited by V. Yevjevich, pp. 165–191, Water Resour. Publ., Fort Collins, Colo.

Nienow, P. W., M. Sharp, and I. C. Willis (1996), Velocity-discharge relationships derived from dye tracer experiments in glacial meltwaters: Implications for subglacial flow conditions, *Hydrol. Processes*, *10*, 1411–1426.

Nienow, P. W., M. Sharp, and I. C. Willis (1998), Seasonal changes in the morphology of the subglacial drainage system, Haut Glacier d'Arolla, Switzerland, *Earth Surf. Processes Landforms*, *23*, 825–843.

Panagopoulos, G., and N. Lambrakis (2006), The contribution of time series analysis to the study of the hydrodynamic characteristics of the karst systems: Application on two typical karst aquifers of Greece (Trifilia, Almyros Crete), *J. Hydrol.*, *329*, 368–376.

Peterson, E. W., and C. M. Wicks (2005), Fluid and solute transport from a conduit to the matrix in a carbonate aquifer system, *Math. Geol.*, *37*, 851–867.

Ponce, V., and D. Simons (1977), Shallow wave propagation in open channel flow, *J. Hydraul. Div. Am. Soc. Civ. Eng.*, *103*, 1461–1476.

Prelovšek, M., J. Turk, and J. Gabrovšek (2008), Hydrodynamic aspect of caves, *Int. J. Speleol.*, *37*, 11–26.

Rossman, L. A. (2005), Storm water management model user's manual: Version 5.0, *Rep. EPA/600/R-05/040*, U.S. Environ. Prot. Agency, Cincinnati, Ohio.

Rossman, L. A. (2006), Storm water management model quality assurance report: Dynamic wave flow routing, *Rep. EPA/600/R-06/097*, U.S. Environ. Prot. Agency, Cincinnati, Ohio.

Saar, M. O., and M. Manga (2003), Seismicity induced by seasonal groundwater recharge at Mt. Hood, Oregon, *Earth Planet. Sci. Lett.*, *214*, 605–618.

Springer, G. S. (2004), A pipe-based, first approach to modeling closed conduit flow in caves, *J. Hydrol.*, *289*, 178–189.

Springer, G. S., and E. E. Wohl (2002), Empirical and theoretical investigations of sculpted forms in Buckeye Creek Cave, West Virginia, *J. Geol.*, *110*, 469–481.

Springer, G. S., E. E. Wohl, J. A. Foster, and D. G. Boyer (2003), Testing for reach-scale adjustments of hydraulic variables to soluble and insoluble strata: Buckeye Creek and Greenbrier River, West Virginia, *Geomorphology*, *56*, 201–217.

Stoker, J. J. (1957), *Water Waves*, Interscience, New York.

Swift, D. A., P. W. Nienow, T. B. Hoey, and D. W. F. Mair (2005), Seasonal evolution of runoff from Haut Glacier d'Arolla, Switzerland and implications for glacial geomorphic processes, *J. Hydrol.*, *309*, 133–148.

Tessier, Y., S. Lovejoy, P. Hubert, D. Schertzer, and S. Pecknold (1996), Multifractal analysis and modeling of rainfall and river flows and scaling, causal transfer functions, *J. Geophys. Res.*, *101*, 26,427–26,440.

Torbarov, K. (1976), Estimation of permeability and effective porosity in karst on the basis of recession curve analysis, in *Karst Hydrology and Water Resources*, vol. 1, edited by V. Yevjevich, pp. 121–136, Water Resour. Publ., Fort Collins, Colo.

White, W. B. (1988), *Geomorphology and Hydrology of Karst Terrains*, Oxford Univ. Press, New York.

Willis, I. C. (1995), Intra-annual variations in glacier motion: A review, *Prog. Phys. Geogr.*, *19*, 61–106.

Willis, I., W. Lawson, I. Owens, B. Jacobel, and J. Autridge (2009), Subglacial drainage system structure and morphology of Brewster Glacier, New Zealand, *Hydrol. Processes*, *23*, 384–396.

Yuhr, L. (2009), Clues to connections: Geophysical analysis to aid in identifying and characterizing flowpaths direct and indirect, paper presented at 5th Conference on Hydrogeology, Ecology, Monitoring, and Management of Ground Water in Karst Terrains, Natl. Ground Water Assoc., Safety Harbor, Fla.

M. D. Covington and M. O. Saar, Department of Geology and Geophysics, University of Minnesota-Twin Cities, 310 Pillsbury Dr. SE, Minneapolis, MN 55455, USA. (covin039@umn.edu)

C. M. Wicks, Department of Geology and Geophysics, Louisiana State University, E-235 Howe-Russell, Baton Rouge, LA 70803, USA.